THE COMPANY OF
Biologists

RESEARCH ARTICLE

Differential activation of natriuretic peptide receptors modulates cardiomyocyte proliferation during development

Jason R. Becker[1],*, Sneha Chatterjee[1], Tamara Y. Robinson[1], Jeffrey S. Bennett[2], Daniela Panáková[3], Cristi L. Galindo[1], Lin Zhong[1], Jordan T. Shin[4], Shannon M. Coy[3], Amy E. Kelly[3], Dan M. Roden[5], Chee Chew Lim[1] and Calum A. MacRae[3]

ABSTRACT

Organ development is a highly regulated process involving the coordinated proliferation and differentiation of diverse cellular populations. The pathways regulating cell proliferation and their effects on organ growth are complex and for many organs incompletely understood. In all vertebrate species, the cardiac natriuretic peptides (ANP and BNP) are produced by cardiomyocytes in the developing heart. However, their role during cardiogenesis is not defined. Using the embryonic zebrafish and neonatal mammalian cardiomyocytes we explored the natriuretic peptide signaling network during myocardial development. We observed that the cardiac natriuretic peptides ANP and BNP and the guanylate cyclase-linked natriuretic peptide receptors Npr1 and Npr2 are functionally redundant during early cardiovascular development. In addition, we demonstrate that low levels of the natriuretic peptides preferentially activate Npr3, a receptor with Gi activator sequences, and increase cardiomyocyte proliferation through inhibition of adenylate cyclase. Conversely, high concentrations of natriuretic peptides reduce cardiomyocyte proliferation through activation of the particulate guanylate cyclase-linked natriuretic peptide receptors Npr1 and Npr2, and activation of protein kinase G. These data link the cardiac natriuretic peptides in a complex hierarchy modulating cardiomyocyte numbers during development through opposing effects on cardiomyocyte proliferation mediated through distinct cyclic nucleotide signaling pathways.

KEY WORDS: ANP, BNP, Npr3, Cardiomyocyte proliferation, Heart development, Natriuretic peptides

INTRODUCTION

The cardiac natriuretic peptides, atrial natriuretic peptide (ANP) and brain (or B-type) natriuretic peptide (BNP), are dynamically regulated in the adult heart and in other tissues by changes in blood pressure and other pathological processes (de Bold, 1985; Sudoh et al., 1988). The active peptides exert paracrine effects on cardiomyocytes and other cell types, as well as endocrine effects on remote organs such as the kidneys, adrenal glands or vasculature. Although cardiac natriuretic peptides are produced at high levels during cardiogenesis, little is known of the fundamental roles of these peptides during this developmental time period (Bloch et al., 1986; Horsthuis et al., 2008; Tanaka et al., 1999; Zeller et al., 1987).

Several murine genetic models have shed light on the role of the natriuretic peptides in the adult mammalian heart. Elimination of individual natriuretic peptide genes leads to significant effects on the post-natal heart, with myocardial hypertrophy in adult animals null for *Nppa* and myocardial fibrosis in older adults null for *Nppb* (John et al., 1995; Tamura et al., 2000). Investigators have attempted to dissect potential redundancies through elimination of Npr1, a particulate guanylate cyclase receptor that is activated by both ANP and BNP. A myocardial-restricted knockout of *Npr1* confirmed that this receptor plays a direct role in blunting the hypertrophic response of adult myocardium (Holtwick et al., 2003), but it was also noted that early post-natal survival was decreased in *Npr1* null mice (Oliver et al., 1997; Scott et al., 2009). These data suggest that the natriuretic peptide pathway is important for cardiac responses to specific stressors, but also infer that the exploration of potential redundancy in murine models may be limited by viability.

The complexity of the natriuretic peptide signaling pathway is further compounded by the interactions of the active peptides with two additional receptors, Npr2 [also known as guanylyl cyclase-B (GC-B)] and Npr3 (also known as Npr-C). Similar to Npr1, Npr2 is also a particulate guanylate cyclase-linked receptor. The role of Npr2 in cardiomyocyte development is poorly understood, but a transgenic rat that overexpressed a dominant-negative isoform of the Npr2 receptor developed cardiac hypertrophy despite a normal systemic blood pressure (Langenickel et al., 2006). Npr3 does not possess guanylate cyclase activity and it is thought to act as a clearance receptor by binding and internalizing circulating natriuretic peptides (Nussenzveig et al., 1990). However, the cytoplasmic domain of this receptor contains Gi activator sequences that cause inhibition of adenylyl cyclase (Anand-Srivastava et al., 1996; Lelièvre et al., 2006; Murthy and Makhlouf, 1999). Deletion of the *Npr3* gene in mouse causes systemic hypotension and skeletal defects (Matsukawa et al., 1999).

By applying knockdown and transgenic techniques in the zebrafish and in mammalian cardiomyocyte cultures, we show a novel role for the cardiac natriuretic peptides in dynamically regulating embryonic and neonatal cardiomyocyte proliferation in a concentration-dependent manner. Low concentrations of natriuretic peptides enhanced proliferation of embryonic zebrafish and neonatal rodent cardiomyocytes through Npr3-dependent modulation of cAMP signaling. By contrast, elevated concentrations of natriuretic peptides inhibit cardiomyocyte proliferation through protein kinase G (PKG)-mediated signaling that is dependent on Npr1 and Npr2. These results demonstrate a novel role for the natriuretic peptides in regulating developmental cardiomyocyte proliferation via the distinctive coupling of the natriuretic peptide receptors to discrete cyclic nucleotide signaling pathways.

[1]Division of Cardiovascular Medicine, Vanderbilt University School of Medicine, Nashville, TN 37235, USA. [2]Center for Human Genetics Research, Vanderbilt University School of Medicine, Nashville, TN 37235, USA. [3]Harvard Medical School and Division of Cardiology, Brigham and Women's Hospital, Boston, MA 02215, USA. [4]Harvard Medical School and Cardiovascular Research Center, Massachusetts General Hospital, Boston, MA 02114, USA. [5]Departments of Medicine and Pharmacology, Vanderbilt University School of Medicine, Nashville, TN 37235, USA.

*Author for correspondence (jason.becker@vanderbilt.edu)

Development

RESULTS

Perturbation of natriuretic peptide levels during embryogenesis reveals a role for these peptides in cardiac development

The full-length sequence of the zebrafish *nppa* was available (NM_198800.2) and we identified and characterized the zebrafish ortholog of the *nppb* gene (supplementary material Fig. S1). Whole-mount *in situ* hybridization analysis of *nppa* and *nppb* was undertaken at various developmental stages (Fig. 1A). The expression of zebrafish *nppb* is similar to that of *nppa*, with more robust expression in the ventricle compared with the atrium. The earliest expression was detected at 24 hours post-fertilization (hpf). We performed quantitative RT-PCR of *nppa* and *nppb* to determine the changes in expression levels during early heart development. Using the 24 hpf measurement as the reference point, *nppa* and *nppb* expression increase 50- and 22-fold, respectively, by 48 hpf. Expression of both genes decreases substantially from 72 hpf to 96 hpf but remain above the 24 hpf levels (Fig. 1B).

We then designed morpholino antisense oligonucleotides to eliminate the translation of the cardiac natriuretic proteins. Morpholino specificity was confirmed using *nppa*:YFP and *nppb*:YFP constructs incorporating the respective oligonucleotide target sequences (supplementary material Fig. S2A,B). The
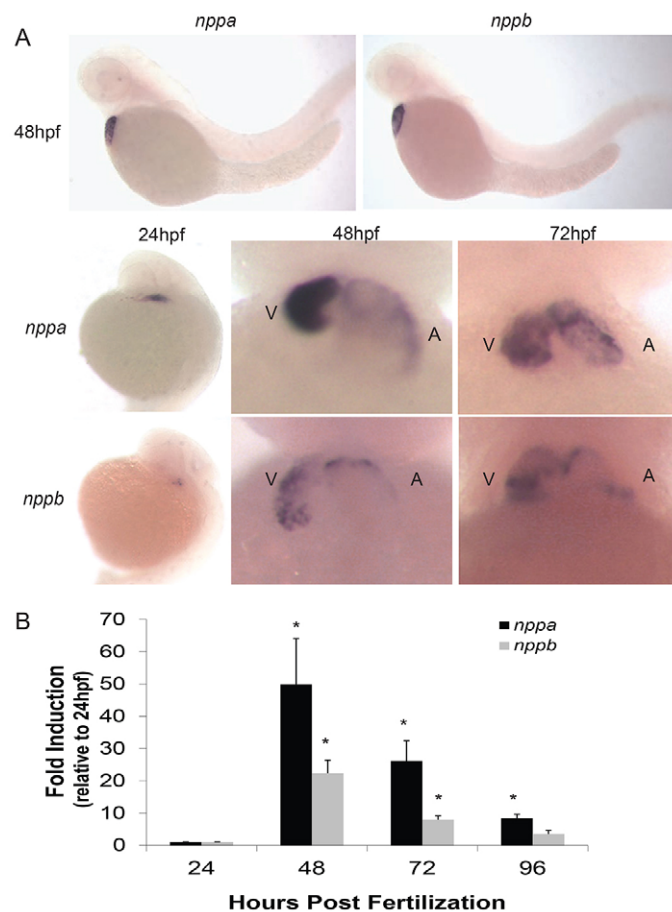
knockdown of either Nppa or Nppb in isolation did not cause any discernible changes in early cardiac development or function. However, when both genes were knocked down simultaneously, we observed a substantial enlargement of the zebrafish heart (Fig. 2A). In addition, we generated a transgenic zebrafish model to overexpress *nppb* using the Gal4:UAS transactivator system (Fig. 2B,D). The overexpression of *nppb* caused the overall zebrafish heart size to decrease substantially (Fig. 2C,D).
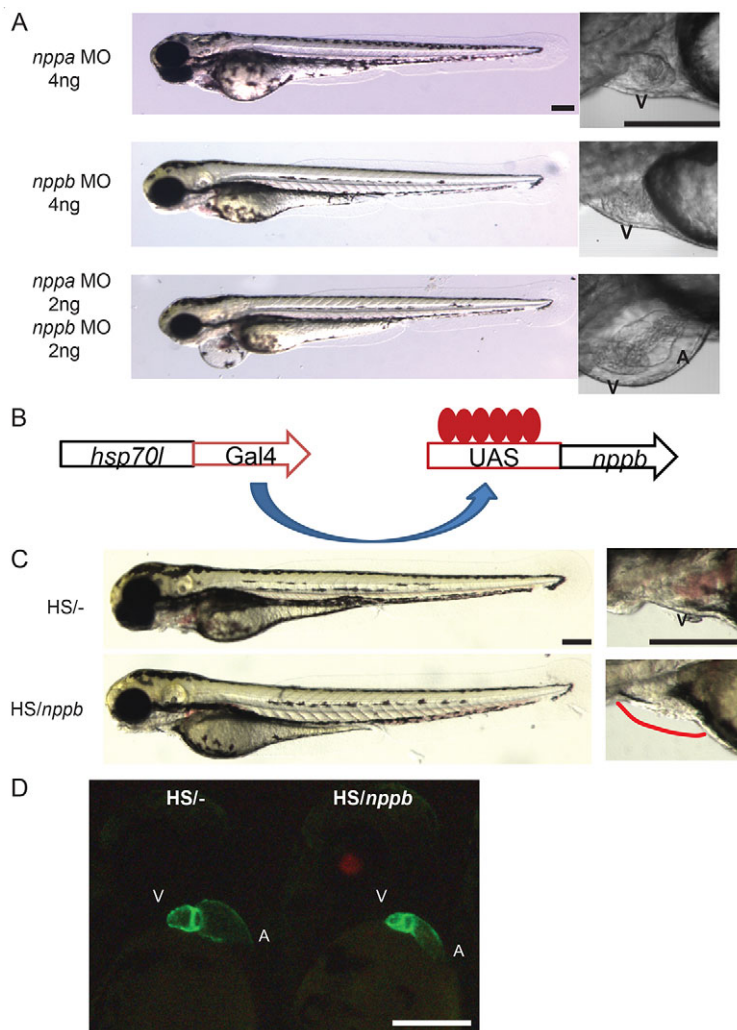
Cardiomyocyte proliferation is modulated by changes in natriuretic peptide levels

To see if changes in cell number might account for the divergent phenotypes seen with reduction or overexpression of the cardiac natriuretic peptides in the embryonic heart, we next counted total cardiomyocytes. The Nppa/Nppb double knockdown embryos exhibited a hyperplastic response with an ~15% increase in total cardiomyocytes at 48 hpf, whereas in the *nppb*-overexpressing embryos there was a 20% reduction in total cardiomyocytes at 48 hpf compared with control embryos (Fig. 3A,B). The overall body length at 48 hpf of both Nppa/Nppb double knockdown and *nppb* overexpression embryos was <5% different from control embryos [control 3146±20, *nppb* overexpression (HS/*nppb*) 3016±26, Nppa/Nppb MO 3109±39 μm; mean ± s.e.m.], suggesting that these effects were not a result of generalized effects on growth. The reduction in total cardiomyocyte numbers was not a result of increased cardiomyocyte apoptosis (Fig. 3C), but was a consequence of significant reduction in cardiomyocyte proliferation (Fig. 3D,E).

Cardiomyocyte cell size was not increased in the Nppa/Nppb double knockdown embryos, which suggests cell hypertrophy was not the primary cause of the larger hearts in the Nppa/Nppb double knockdown embryos (supplementary material Fig. S2D,E). However, the cell size was decreased in the *nppb* overexpression embryos compared with controls, suggesting that both reduced cardiomyocyte proliferation and size are contributing to the reduced overall heart size in HS/*nppb*.

To confirm that the effects of the cardiac natriuretic peptides were independent from any extra-cardiac or systemic actions of the natriuretic peptides, we measured proliferation in the H9C2 cardiomyocyte cell line and neonatal rat cardiomyocyte primary cell cultures. Rat and mouse ventricular cardiomyocytes retain the capacity to proliferate for ~96 hours post-natally if cultured in high serum conditions (Fig. 4A,B; supplementary material Fig. S3A,B) (Hammoud et al., 2009; Kerkela et al., 2008; Li et al., 1996; McKoy et al., 2007). This allowed us to assess accurately the effects of natriuretic peptide concentrations on mammalian neonatal cardiomyocyte proliferation. We found that low concentration natriuretic peptide supplementation increased the baseline rates of proliferation of H9C2 cells by 11% and neonatal cardiomyocytes by up to 27%, whereas high concentration natriuretic peptide supplementation decreased proliferation by up to 18% for H9C2 cells (supplementary material Fig. S3C) and 24% for neonatal cardiomyocytes (Fig. 4C). Fluorescence-activated cell sorting analysis of annexin V-, terminal deoxynucleotidyl transferase dUTP nick end labeling (TUNEL)- and propidium iodide-stained neonatal rat ventricular myocytes (NRVMs) confirmed that the changes in total cell populations were not a result of changes in cell viability (Fig. 4D,E).

Although H9C2 cardiomyocytes are a homogenous cell population, primary cultures of neonatal cardiomyocytes can be contaminated by non-myocytes. Therefore, to confirm our results we directly measured the number of cardiac troponin T (Tnnt2)-positive cells that progressed through the S phase of the cell cycle by

Fig. 1. Developmental induction of cardiac natriuretic peptides peaks at 48 hpf in the embryonic zebrafish. (A) Whole-mount *in situ* hybridization of *nppa* and *nppb* zebrafish embryos. A, atrium; V, ventricle. (B) Quantitative RT-PCR measurement of *nppa* and *nppb* during different developmental time points. Data are expressed as mean + s.e.m. *P<0.05, relative to 24 hpf values.

Fig. 2. Altered cardiac natriuretic expression changes heart growth *in vivo*. (A) Morpholino knockdown of Nppa or Nppb in isolation or simultaneously. Heart enlargement was seen in the Nppa/Nppb double knockdown embryos but was absent in single knockdown morphants (72 hpf). (B) Inducible Gal4/UAS transactivator system to overexpress *nppb in vivo*. (C) The *nppb* overexpression embryos (HS/*nppb*) had a large reduction of pericardial fluid volume (magnified panel, red line details normal pericardial border) but overall embryonic growth was minimally altered (72 hpf). (D) The *cmlc2*/CFP fluorescent marker was utilized to visualize the chamber dimensions better in control (HS/-) and *nppb* overexpression (HS/*nppb*) embryos (48 hpf). The ventricular and atrial sizes were both reduced in *nppb* overexpression embryos. Red fluorescent marker in lens denotes UAS/*nppb* carrier status. A, atrium; V, ventricle. Scale bars: 200 μm.

measuring the incorporation of the thymidine analog 5-ethynyl-2′-deoxyuridine (EdU) (supplementary material Fig. S3D). This enabled us to confirm that the changes in cell numbers seen in the cardiomyocyte cultures resulted from changes in cardiomyocyte proliferation. We found an increased number of EdU-positive cardiomyocytes in the low concentration (10 nM ANP exposure) group and a lower number of EdU-positive cardiomyocytes in the high concentration (10 μM ANP exposure) group (Fig. 4F). In addition, the proportion of EdU-positive cells that were binucleate was <6% in all three treatment groups, supporting the conclusion that the primary effect measured was cell division and not just karyokinesis.

Natriuretic peptide effects on cardiomyocyte number are mediated via the three natriuretic peptide receptors

In order to define the mechanisms through which the natriuretic peptides exert their effects *in vivo*, we identified the zebrafish orthologs of Npr1, Npr2 and Npr3 and found that all three receptors are expressed in zebrafish cardiac tissue (supplementary material Fig. S4A,B). In contrast to *nppa* and *nppb*, the expression of the natriuretic peptide receptors did not increase as dramatically through the early stages of heart development (supplementary material Fig. S4B). However, *npr3* expression did surge at 48 hpf coinciding with peak expression of *nppa* and *nppb* in early zebrafish heart development.

As *npr1* and *npr2* both exhibit guanylate cyclase activity, we investigated if the knockdown of these receptors could phenocopy the Nppa/Nppb double knockdown morphants. We designed morpholinos to disrupt the normal splicing of these genes to generate transient loss of function (supplementary material Fig. S4C,D). To compare the different groups directly, we used *cmlc2*:CFP labeling of the embryonic heart and estimated heart dimensions in all of the different experimental groups at the same time point during development (48 hpf) (Fig. 5A,B). When *npr1* or *npr2* alone were targeted, there were minimal changes in early cardiac morphogenesis or physiology. However, simultaneous disruption of both *npr1* and *npr2* resulted in perturbation of cardiac chamber formation comparable to that observed in the Nppa/Nppb double knockdown embryos.

Next, we injected the *npr1* and *npr2* morpholinos into HS:*nppb* transgenic embryos. The decreased heart size observed in HS:*nppb* embryos was prevented by simultaneous knockdown of *npr1* and *npr2*, suggesting that the effects of *nppb* overexpression are mediated via Npr1 and Npr2 activation (Fig. 5A,B). Importantly, it was also possible to block the effects of *nppb* overexpression using the cognate *nppb* translation-blocking morpholino.

After selectively targeting the particulate guanylate cyclase-linked natriuretic peptide receptors *npr1* and *npr2*, we then performed a morpholino knockdown of *npr3* (supplementary material Fig. S4E). We found that embryos injected with the *npr3* morpholino
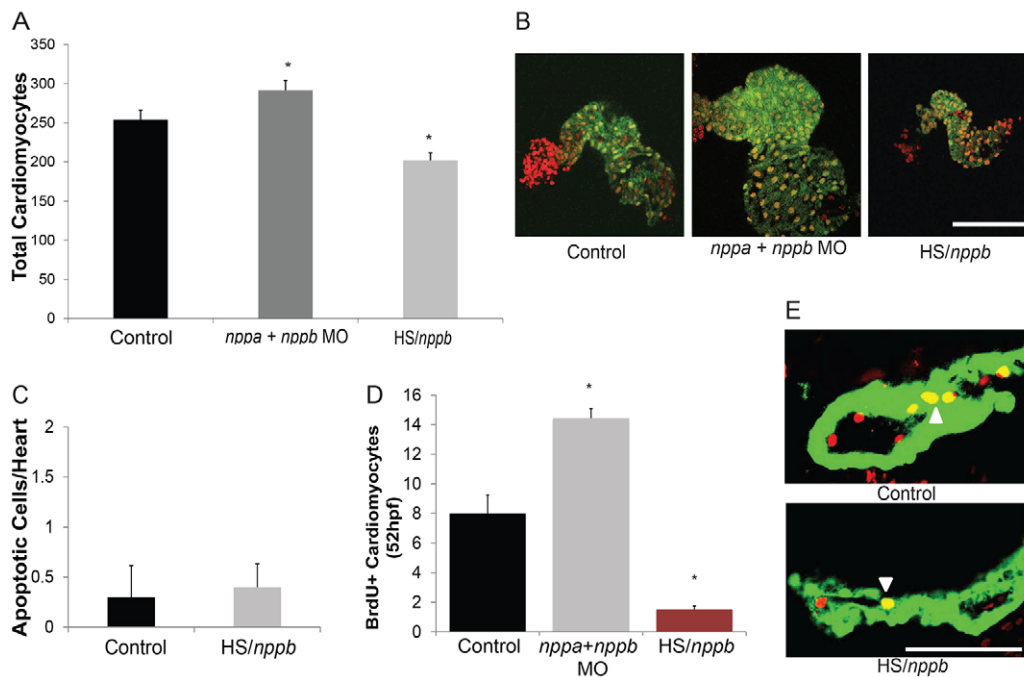
Fig. 3. Manipulation of cardiac natriuretic peptide expression alters total cardiomyocyte numbers in the embryonic heart. (A) Total cardiomyocytes at 48 hpf were increased in the Nppa/Nppb double knockdown (*nppa/nppb* MO) embryos, but were decreased in the *nppb* overexpression embryos (HS/*nppb*). *$P<0.02$ compared with control. (B) Representative images from *cmlc2*:CFP (pseudo-colored green) and DAPI (pseudo-colored red) stained hearts. (C) The total number of apoptotic heart cells was not increased in the *nppb* overexpression embryos. $P>0.05$ compared with control. (D) Knockdown of Nppa/Nppb and overexpression of *nppb* were able to significantly alter cardiomyocyte proliferation at 52 hpf. *$P<0.03$ compared with control. (E) Representative images of BrdU-labeled (red) cmlc2:CFP (green)-positive heart tissue. White arrowhead indicates BrdU-positive cardiomyocytes. Intracavitary BrdU+ cells were considered to be endothelial in origin and were not counted. All data are expressed as mean + s.e.m. Scale bars: 100 µm.

developed at a normal rate except that their overall heart sizes were smaller than control embryos at 48 hpf (Fig. 5A,B). The Npr3 knockdown embryos had very similar heart size and morphology to HS/*nppb* embryos.

We then measured cardiomyocyte proliferation in embryos lacking the natriuretic peptide receptors. We found that embryos lacking the particulate guanylate cyclase natriuretic peptide receptors *npr1* and *npr2* displayed increased levels of cardiomyocyte proliferation. However, embryos lacking *npr3* exhibited reduced embryonic cardiomyocyte proliferation (Fig. 5C). We also evaluated the addition of cardiomyocytes to the arterial pole of the zebrafish ventricle from 30 to 48 hpf to determine if disruption of natriuretic peptide signaling in the embryonic heart was perturbing differentiation of cardiomyocyte progenitors. In all three groups, new ventricular cardiomyocytes were added to the arterial pole of the ventricle (identified by green cells indicating non-photoactivated kaede), which suggests that our observations are not a result of altered proliferation in progenitor compartments outside the primary heart field, but rather of differentiated ventricular cardiomyocytes (Fig. 5D).

We also measured expression of *nppa*, *nppb*, *npr1*, *npr2* and *npr3* when there was knockdown or overexpression of different components of the cardiac natriuretic peptide signaling pathway (supplementary material Fig. S5). When there was knockdown of Nppa/Nppb or Npr1/Npr2 there was a robust increase in *nppa/nppb* expression (greater than fourfold increase). By contrast, Npr3 knockdown caused a reduction in *nppa* and *nppb* expression (60% and 23% reduction, respectively). Overexpression of *nppb* caused a modest but significant reduction of *npr1*. Lastly, the efficacy of our splice-targeting morpholinos (*npr1*, *npr2*, *npr3*)

was also confirmed with reduction of the target transcripts of >95%.

The inhibitory effects of natriuretic peptides on cardiomyocyte proliferation are mediated via activation of PKG

We then utilized mammalian cardiomyocyte primary culture to explore further the downstream signaling pathways involved in natriuretic peptide suppression of cardiomyocyte proliferation. First, we verified that all three natriuretic peptide receptors are expressed in mammalian cardiomyocytes at different stages of heart development (supplementary material Fig. S6A). This was performed by analyzing publicly available microarray datasets collected in the Gene Expression Omnibus (National Library of Medicine) (n=3-10 biological replicates/group). We found that *Npr1*, *Npr2* and *Npr3* were all expressed in embryonic, neonatal and adult murine cardiomyocytes at levels similar to the beta-1 adrenergic receptor (*Adrb1*) (a receptor highly expressed in cardiomyocytes). Of note, *Npr2* was expressed at higher levels in neonatal and adult cardiomyocytes than *Npr1* ($P<0.001$). The cardiomyocyte sarcomeric protein, cardiac troponin T (*Tnnt2*), was used to verify the accuracy of the cardiomyocyte expression data.

We then tested to see if Npr1 and Npr2 were biologically active in primary cardiomyocyte cell culture using selective peptide agonists. Dendroaspis natriuretic peptide (DNP, an Npr1-selective agonist) and C-type natriuretic peptide (CNP, an Npr2-selective agonist) were each able to inhibit neonatal cardiomyocyte proliferation at elevated concentrations (10 µM CNP and 1 µM DNP) in a manner similar to ANP 10 µM (supplementary material Fig. S6B,C). This confirmed that Npr1 and Npr2 were functionally
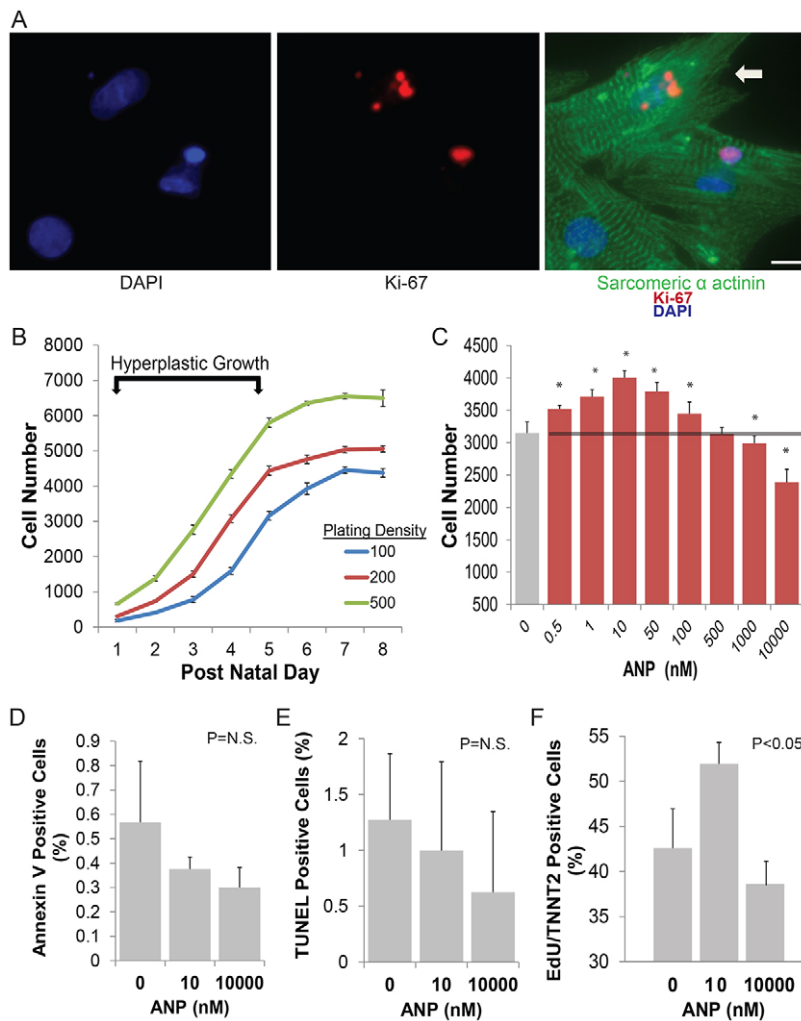
Fig. 4. Manipulating natriuretic peptide concentrations can modulate mammalian cardiomyocyte proliferation. (A) Example of rat neonatal cardiomyocytes undergoing karyokinesis using Ki-67 marker (red) and sarcomeric alpha actinin (green). White arrow denotes area of sarcomere disassembly in preparation for cell division. (B) Measurement of cell proliferation in P1 to P8 rat ventricular cardiomyocytes shows an early hyperplastic phase of cellular growth followed by a cessation of cell proliferation independent of initial plating density. Data are mean ± s.d. (C) Proliferating NRVMs show a concentration-dependent effect of ANP on cardiomyocyte proliferation over 48 hours. *$P<0.0001$ compared with control. Data are expressed as mean + s.d. (D,E) Low or high concentration ANP does not increase NRVM apoptosis (annexin V or TUNEL labeling). $P>0.05$ (N.S., not significant). (F) NRVM proliferation measured by EdU incorporation confirmed that low concentration ANP (10 nM) enhanced NRVM proliferation whereas high concentration ANP (10 μM) suppressed NRVM proliferation. $P<0.05$. Data expressed as mean + s.e.m. Scale bar: 50 μm.

active in mammalian cardiomyocytes and contributed to the inhibition of cardiomyocyte proliferation seen with high concentrations of natriuretic peptides.

Activation of Npr1 and Npr2 leads to increased cGMP levels, which in turn result in the activation of PKG. We targeted PKG with selective inhibitors to determine if this kinase contributed to the natriuretic peptide effect on cardiomyocyte proliferation (Fig. 6A). We first used Rp-cGMP and were able to almost eliminate the inhibitory effects of high concentration ANP on cardiomyocyte proliferation. We then employed a second selective PKG inhibitor, KT5823, and prevented the reduced cardiomyocyte proliferation seen with high concentration ANP exposure. In fact, cardiomyocyte proliferation rates were similar to those observed with low concentration ANP, suggesting that complete blockade of PKG allowed the proliferative effects of Npr3 activation by ANP to be unmasked even in the setting of high concentration ANP. Of note, both selective PKG inhibitors were used at a concentration that did not alter baseline cardiomyocyte proliferation (supplementary material Fig. S6D).

Finally, the direct application of 8-pCPT-cGMP (a cell-permeable analog of cGMP that activates PKG) mimicked the inhibitory effect of high concentrations of ANP on NRVM proliferation (Fig. 6B). These data suggest that cGMP activation of PKG mediates the anti-proliferative effects of high concentration ANP signaling through Npr1 and Npr2.

Enhanced proliferation of cardiomyocytes at low concentrations of natriuretic peptides is mediated by activation of Npr3 and cAMP pathways

To verify that Npr3 was involved in the induction of cardiomyocyte proliferation observed with low concentrations of ANP, we used the selective Npr3 antagonist AP-811 (Veale et al., 2000; William et al., 2008). Although AP-811 did not alter baseline cardiomyocyte proliferation across a wide range of concentrations (supplementary material Fig. S7A), when we exposed proliferating cardiomyocytes to low concentration ANP (10 nM) in the setting of an Npr3 antagonist, the increased cell proliferation was blocked (Fig. 6C). In contrast to PKG inhibition, blocking Npr3 had minimal effects on the anti-proliferative actions of high concentration ANP. We then combined Npr3 antagonism with AP-811 and PKG inhibition with KT5823 and found that we could completely block the effects of ANP on cardiomyocyte proliferation (supplementary material Fig. S7A).

To determine if Npr3 inhibition of adenylate cyclase was playing a role in cardiac proliferation, we tested whether direct inhibition of adenylate cyclase could mimic the proliferative effects of low concentration ANP. We exposed neonatal rat cardiomyocytes to the selective adenylate cyclase inhibitor SQ 22536 and found that proliferation could be enhanced by adenylate cyclase inhibition in a concentration-dependent manner (Fig. 6D; supplementary material Fig. S7B), mimicking the low concentration ANP activation of
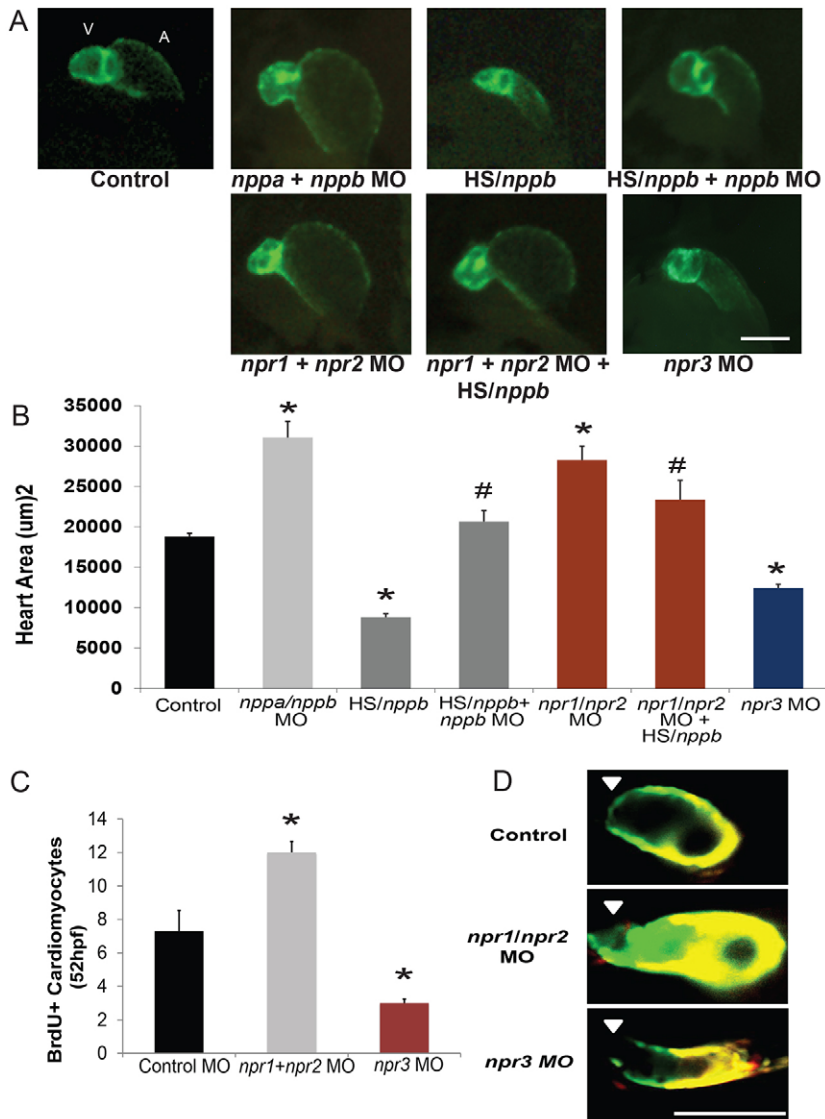
Fig. 5. The cardiomyocyte proliferation effects of the cardiac natriuretic peptides are coordinated by the action of multiple natriuretic peptide receptors *in vivo*. (A) Lateral views of 48 hpf *cmlc2*:CFP embryos show significantly altered atrial and ventricular chamber sizes in Nppa/Nppb double knockdown and *nppb* overexpression embryos. Likewise, double knockdown of both natriuretic peptide guanylate cyclase-linked receptors, Npr1 and Npr2, caused a similar phenotype as the Nppa/Nppb double knockdown and could block the effect of *nppb* overexpression (*npr1*/*npr2* MO + HS/*nppb*). Finally, the knockdown of Npr3 caused a significant reduction in both atrial and ventricular chamber sizes that was similar to that observed after overexpression of *nppb*. (B) Corresponding heart surface areas of all treatment groups shown in A. *$P<0.05$ compared with control heart size, #$P<0.05$ compared with HS/*nppb* alone. (C) Cardiomyocyte proliferation was increased in the Npr1 and Npr2 knockdown embryos, whereas Npr3 knockdown embryos had reduced cardiomyocyte proliferation at 52 hpf as assessed by BrdU labeling of cardiomyocytes. *$P<0.01$ compared with control. (D) Differentiation of ventricular cardiomyocytes between 30 and 48 hours of heart development was not altered by knockdown of the natriuretic peptide receptors. White arrowhead denotes arterial pole, areas of green tissue were added after 30 hpf (non-photoconverted). Yellow tissue is a mixture of photoconverted red tissue and non-photoconverted green tissue. All data are expressed as mean + s.e.m. Scale bars: 100 μm.

Npr3. Conversely, the addition of a cAMP analog (8-Br-cAMP) could block the enhanced proliferation of cardiomyocytes seen with low concentrations of ANP in a concentration-dependent manner (Fig. 6D; supplementary material Fig. S7B). We then explored the effects of activation of adenylyl cyclase on cardiomyocyte proliferation. We used the β-adrenergic receptor agonist isoproterenol to activate adenylyl cyclase and found that cardiomyocyte proliferation was decreased (supplementary material Fig. S8). We found that we could block the effect of adenylyl cyclase activation by simultaneous addition of low concentration ANP (10 nM). Conversely, the reduced cardiomyocyte proliferation seen with high concentration ANP (10 μM) was enhanced in the setting of adenylyl cyclase activation by isoproterenol.

Finally, we performed siRNA knockdown of Npr3 in NRVMs. When Npr3 was eliminated using siRNA we were able to completely block the enhanced proliferation and DNA synthesis seen with low concentration ANP (Fig. 7A,B). In addition, we performed direct measurement of EdU-positive cardiomyocytes using fluorescence microscopy to confirm that DNA synthesis was indeed reduced compared with control cells stimulated with 10 nM ANP (Fig. 7C,D).

DISCUSSION
In the work we have outlined, we establish a novel role for the cardiac natriuretic peptides in modulating cardiomyocyte proliferation during cardiogenesis by differentially activating the guanylate cyclase-linked natriuretic peptide receptors (Npr1 and Npr2) and Npr3 (a clearance receptor and activator of Gi subunit). Our data establish in both a zebrafish model and in proliferating mammalian cardiomyocytes, that the natriuretic peptides modulate cardiomyocyte division in a concentration-dependent manner. Low concentrations of natriuretic peptide increase cardiomyocyte proliferation whereas high concentrations of these same peptides inhibit cardiomyocyte proliferation. The enhanced proliferation seen with low levels of cardiac natriuretic peptides is primarily mediated through Npr3, whereas the inhibition of proliferation seen with high concentrations of natriuretic peptides is mediated through Npr1 and Npr2 (Fig. 8).

Natriuretic peptides are dynamically expressed during heart development in both zebrafish and mammals (Bloch et al., 1986; Zeller et al., 1987). In our zebrafish model, the experimental results suggest that the surge of natriuretic peptides that occurs at 48 hpf reduces the proliferative capacity of differentiated cardiomyocytes
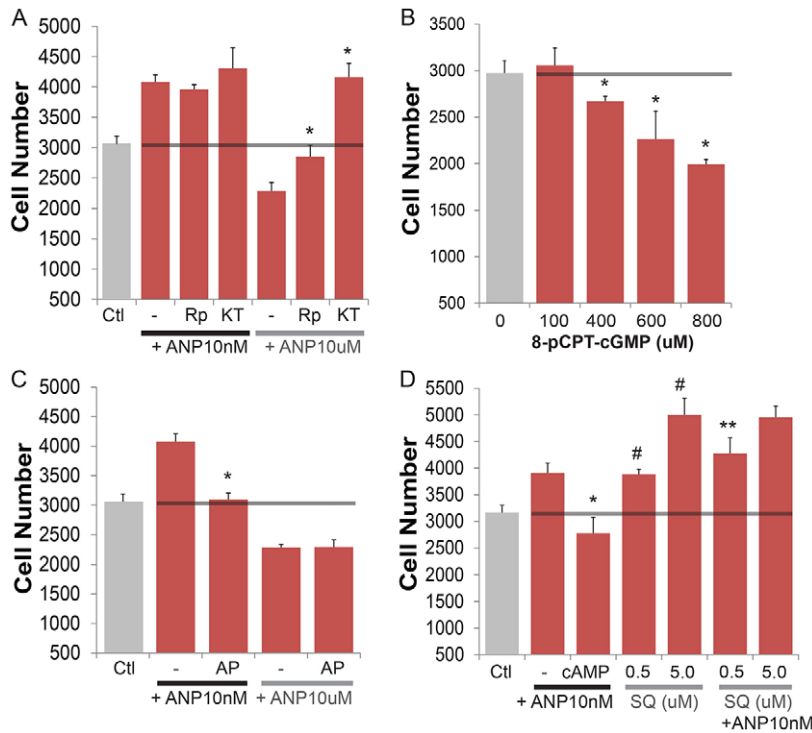
Fig. 6. The concentration-dependent effect of cardiac natriuretic peptides on cardiomyocyte proliferation is controlled by both cGMP and cAMP signaling pathways. (A) The reduced cardiomyocyte proliferation seen with high concentration ANP (10 μM) can be blocked by inhibiting PKG using either Rp-8-pCPT-cGMP (Rp) or KT5823 (KT). *$P<0.01$ compared with 10 μM ANP alone. (B) The addition of cell-permeable cGMP showed a concentration-dependent reduction of cardiomyocyte proliferation. *$P<0.02$ compared with control (0 nM). (C) The Npr3-specific antagonist AP-811 could completely abolish the enhanced cardiomyocyte proliferation seen with low concentration ANP (10 nM). Antagonizing Npr3 had no effect on the reduced cardiomyocyte proliferation seen with high concentration ANP (10 μM). *$P<0.01$ compared with ANP 10 nM alone. (D) Addition of cAMP could abolish the enhanced proliferation seen with low concentration ANP (10 nM). Direct inhibition of adenylyl cyclase with SQ 22536 (SQ) can mimic the enhanced proliferation seen with low concentration ANP (10 nM). Combination of low concentration ANP (10 nM) and 0.5 μM SQ showed an additive effect on proliferation. However, adding low concentration ANP to 5.0 μM SQ showed no increased benefit. *$P<0.01$ compared with ANP 10 nM alone; #$P<0.01$ compared with control; **$P<0.02$ compared with SQ 0.5 μM. Data are expressed as mean + s.e.m.

at that time point. When the translation of *nppa* and *nppb* was reduced during that time period, cardiomyocyte proliferation was increased. Conversely, if *nppb* expression was increased during that time period there was a further reduction of cardiomyocyte proliferation below baseline proliferation rates. The production of cardiac natriuretic peptides decreases substantially by 96 hpf in the developing zebrafish (Fig. 1B), which also coincides with an increase of cardiomyocyte proliferation in the zebrafish heart (Choi et al., 2013). The *in vivo* role of natriuretic peptides during later stages of cardiac development cannot be readily studied in the

embryonic zebrafish; however, murine models lacking or overproducing natriuretic peptides will enable further exploration of the *in vivo* role of these peptides at later developmental time points.

Both Npr1 and Npr2 are expressed in cardiomyocytes during mammalian heart development (supplementary material Fig. S6A) and cardiac natriuretic peptides can activate these receptors at low nanomolar concentrations or less (Johns et al., 2007; Nir et al., 2001; Suga et al., 1992). By contrast, Npr3, which binds all natriuretic peptides, does not exhibit guanylate cyclase activity, but can act as a clearance receptor and can activate Gi, which inhibits adenylyl
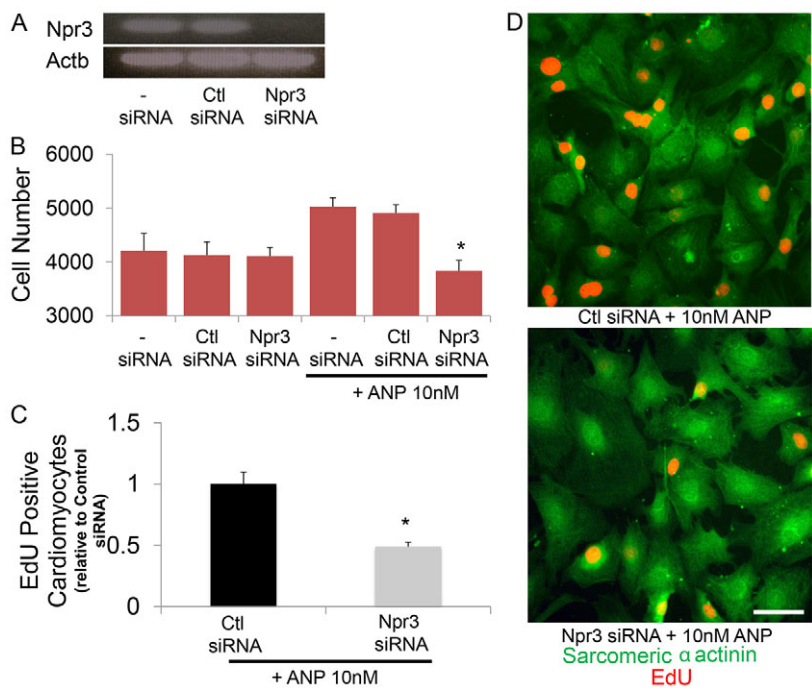
Fig. 7. Knockdown of Npr3 in proliferating neonatal mammalian cardiomyocytes. (A) Npr3 expression was completely abolished by targeted siRNA. (B) The increased cardiomyocyte proliferation caused by low concentration ANP (10 nM) exposure could be completely abolished by siRNA knockdown of Npr3. (C) EdU labeling of sarcomeric alpha actinin-positive cells confirms that Npr3 knockdown could block the effect of low concentration ANP on cell proliferation. *$P<0.03$ compared with control. (D) Representative images of EdU-labeled proliferating cardiomyocytes exposed to low concentration ANP with normal Npr3 expression (top) or lacking Npr3 expression (bottom). Data are expressed as mean + s.e.m. Scale bar: 100 μm.
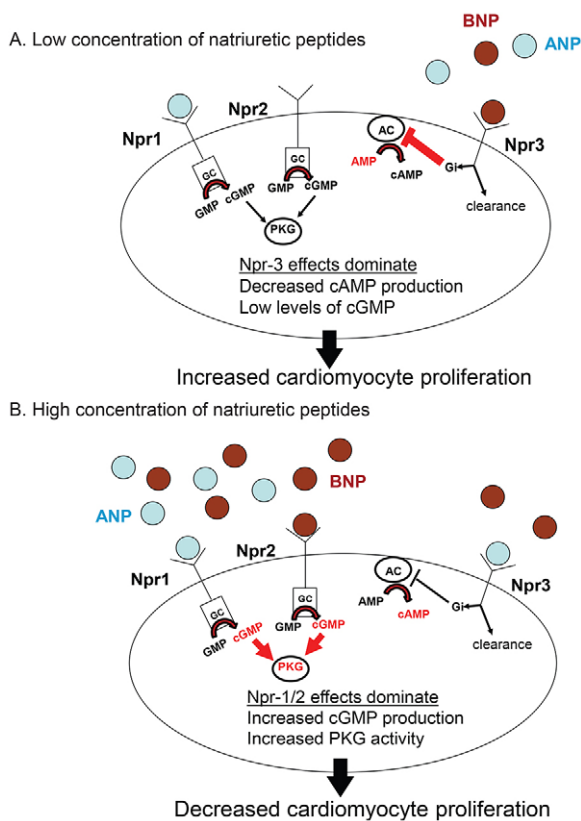
Fig. 8. Concentration-dependent effect of cardiac natriuretic peptides on cAMP and cGMP signaling pathways regulate cardiomyocyte proliferation. (A) The enhanced cardiomyocyte proliferation seen with low concentrations of cardiac natriuretic peptides is primarily mediated through activation of Npr3 and the inhibition of adenylyl cyclase. (B) The inhibition of cardiomyocyte proliferation seen with high concentrations of natriuretic peptides is primarily mediated through Npr1 and Npr2 and the activation of PKG.

cyclase activity and lowers cAMP levels (Anand-Srivastava et al., 1996; Lelièvre et al., 2006; Murthy and Makhlouf, 1999). Our *in vitro* data suggests that at low concentrations of natriuretic peptides, Npr3 effects predominate and cardiomyocyte proliferation is enhanced at least partly through reduction of intracellular cAMP levels. Because we are not able to disrupt Npr3 function in a tissue-specific manner in our zebrafish model, the reduced cardiomyocyte proliferation seen in the zebrafish Npr3 knockdown embryos is likely to be secondary to the elimination of both Npr3 functions (Gi activator and natriuretic peptide clearance). When the concentration of natriuretic peptides increases, Npr1 and Npr2 activation and cGMP/PKG signaling overtake the actions of Npr3. The inhibitory role of natriuretic peptides on cardiomyocyte proliferation through a cGMP-mediated pathway is supported by previous work in fetal sheep cardiomyocytes (O'Tierney et al., 2010). *In vivo* cell type-restricted elimination of Npr3 will help further define its role in cardiomyocyte proliferation by disassociating the cell-specific effects of this receptor (adenylyl cyclase inhibition) from its role as a modulator of systemic natriuretic peptide levels (clearance role).

The role of Npr3 in modulating cellular proliferation has recently been explored in other cell types and it was found that endothelial cell proliferation was augmented by activation of Npr3 whereas smooth muscle cell proliferation was inhibited by Npr3 activation (Khambata et al., 2011). As the mammalian heart is composed of a heterogeneous mixture of different cell types it will be necessary to

determine how the endogenous production of cardiac natriuretic peptides and their receptors regulate the proliferation of these distinctive cell types during cardiogenesis *in vivo*. In addition, it was shown in mammalian smooth muscle cells that knockdown of Npr1 increased the expression of Npr3, which suggests that cellular pathways exist that regulate the coordinated expression of these receptors (Li et al., 2012). We did not see the same coordinated regulation of Npr1 and Npr3 expression in our *in vivo* zebrafish model system, but we did see potential feedback regulation of *nppa/nppb* transcription in our targeted knockdown models.

Together, our data demonstrate that both *in vitro* and *in vivo* the total number of cardiomyocytes is regulated by the differential activation of the natriuretic peptide receptors across a range of natriuretic peptide concentrations. Our data strongly suggest that constitutive low-level expression of the cardiac natriuretic peptides may act to enhance baseline cardiomyocyte proliferation during cardiogenesis, whereas increased expression may act as an effective brake on cardiomyocyte proliferation in the setting of more profound growth stimuli. In conclusion, we have shown a novel role for the cardiac natriuretic peptides in modulating cardiomyocyte proliferation by regulating multiple cyclic nucleotide signaling pathways in a concentration-dependent fashion. A further understanding of how these endogenous cardiac hormones regulate the growth characteristics of cardiomyocytes will enhance our understanding of the mechanisms regulating cardiac growth during development and beyond, in health and disease.

MATERIALS AND METHODS
Cloning of zebrafish *nppb*, *npr1a* and *npr2* genes
Utilizing existing databases (Ensembl, NCBI) we identified the zebrafish orthologs of *Nppb*, *Npr1* and *Npr2* genes. We performed RACE experiments (Ambion) to determine the coding sequence of each gene.

Whole-mount *in situ* hybridization analysis
nppa and *nppb* cDNA constructs were cloned into pDonr221 or pCR8 (Invitrogen) and then subcloned into pCSDest (kindly provided by Nathaniel Lawson, University of Massachusetts). Digoxigenin (dig)-labeled sense and antisense probes were generated and purified (Roche). Control and experimental embryos were fixed in 4% paraformaldehyde (PFA) at 25°C for 2 hours, and then stored in 100% methanol at −20°C until beginning of rehydration protocol. Embryos were rehydrated in PBST (0.1% Tween in PBS), and briefly incubated with proteinase K (4-8 minutes depending on age) and then re-fixed. Hybridization with dig-labeled probe was performed for 12 hours at 65°C. After washes and re-equilibration in PBST, embryos were incubated with anti-Dig antibody (1:5000; Roche, 11093274910) for 12 hours at 4°C, washed, and then staining was performed. Full protocol is outlined in Thisse and Thisse (Thisse and Thisse, 2008).

Gene knockdown *in vivo*
Morpholinos (Gene Tools) were resuspended in 1× Danieu's solution and 125-500 μM (2 nl drop size, 1.9-7.6 ng) of morpholino was injected into fertilized eggs from TuAB fish at the single-cell stage. The *nppa* and *nppb* translation-inhibiting morpholino specificity was evaluated using modified *nppa*:YFP and *nppb*:YFP constructs as described in supplementary material Fig. S2. The *npr1a*, *npr2* and *npr3* morpholinos were splice-targeting morpholinos and their effectiveness is detailed in supplementary material Figs S4 and S5. As an additional measure of morpholino specificity, we tested all of the morpholinos listed below in a *p53* (*tp53*) null zebrafish line to verify that the phenotypes seen in wild-type embryos were not secondary to non-specific activation of p53 (Robu et al., 2007). See supplementary material Table S1 for morpholino sequences.

Gene knockdown *in vitro*
Control siRNA (Invitrogen, 4390843) and Npr3 siRNA (Invitrogen, s129528) were resuspended in siRNA buffer (Dharmacon). Neonatal cardiomyocytes

were transfected with 5 nM of siRNA using DharmaFECT reagent (Thermo Scientific) and the media was changed daily. After 48 hours of siRNA exposure, measurement of the target RNA was performed to verify knockdown efficiency. For all proliferation experiments, an additional 48 hours of siRNA exposure was performed with or without the addition of ANP and cell numbers were measured using the methods described below.

Quantitative RT-PCR

Quantitative RT-PCR was performed using RNA extracted from whole embryos or heart tissue using Trizol reagent (Invitrogen) and reverse transcribed with the QuantiTect Reverse Transcription Kit (Qiagen). Gene specific primers and Sybr Green reagent (Applied Biosystems) were utilized to perform the PCR portion of the experiment. The 2–ΔΔCt method was used to normalize the gene of interest to the endogenous housekeeping gene *eef1a1l1*. See supplementary material Table S1 for primer sequences.

Overexpression of *nppb in vivo*

The pCH:Gtwy:G4VP16 and pBH:UAS:Gtwy:YFP vectors (kindly provided by Michael Nonet, Washington University St Louis, MO, USA) were utilized to make stable transgenic zebrafish lines. The pBH-UAS-Gtwy-YFP vector was modified by removal of the YFP sequence and replacement of the *cmlc2* (*myl7* – Zebrafish Information Network) promoter with a *Xenopus* crystallin promoter to drive mCherry expression in the lens of the eye; this new vector is referred to as pBE-UAS-Gtwy. The zebrafish *nppb* cDNA and 1.5-kb heat shock (HS) 70 promoter were first recombined into pDonr221 (Invitrogen) using BP clonase (Invitrogen). Then LR clonase-mediated recombination was used to place the HS promoter upstream of the Gal4VP16 site in pCH:Gtwy:G4VP16, creating pCH:HS:G4VP16. Likewise, the pDonr:*nppb* construct was recombined using LR clonase to create pBE:UAS:*nppb*. Single-cell embryos were injected with 25 ng/nl vector DNA and 25 ng/nl of Tol2 transposase RNA. Stable transgenics were selected for and outbred for two generations. Adult pCH:HS:G4VP16 and pBE:UAS:*nppb* were then crossed and embryos were collected. The embryos were stored in a 28°C incubator. At 24 hpf, the embryos were placed in a 37°C incubator for 60 minutes, and then returned to a 28°C incubator. At 48 hpf, the embryos were analyzed. Embryos positive for both the *cmlc2*:CFP (Gal4+) and *crystallin*:mCherry (UAS:*nppb*+) fluorescent markers were shown to be positive for ectopic *nppb* expression using whole-mount *in situ* analysis for *nppb*. Embryos containing only *cmlc2*:CFP or crystallin:mCherry did not have ectopic *nppb* expression (supplementary material Fig. S2C).

Cardiac chamber cross-sectional area

All embryos carried a *cmlc2*:CFP or *cmlc2*:GFP cardiomyocyte marker to delineate the atrial and ventricular chambers. At 48 hpf, a lethal dose of tricaine was applied to the embryos causing cessation of myocardial contraction and uniform myocardial relaxation. The embryos were then positioned in the left lateral decubitus position and imaged using a fluorescence dissecting microscope (Zeiss Stereo Discovery v8, AxiocamMRm camera). Once the images were acquired they were analyzed using ImageJ software (NIH) to determine the chamber cross-sectional area of the atrium and ventricle.

Cell size quantification

Control, *nppa*/*nppb* knockdown and *nppb* overexpression embryos were euthanized, their hearts were excised, and then fixed in 4% PFA for 12 hours at 4°C. They were then transferred to 100% methanol and stored at −20°C. The hearts were then rehydrated in PBST. After rehydration, the hearts were washed in a blocking buffer (2 mg/ml bovine serum albumin, 2% goat serum, 1% DMSO in PBST) for 2 hours at 25°C. They were then incubated with mouse anti-zn8 [Developmental Studies Hybridoma Bank (DSHB)] at 1:50 at 4°C for 12 hours, and then Alexa 488 (Invitrogen) at 1:1000 for 3 hours at 25°C. Hearts were imaged using a Zeiss LSM5 Pascal confocal microscope. ImageJ (NIH) analysis software was used to measure the cell surface area of the cardiomyocyte.

Cell culture

Proliferating H9C2 cells were cultured following standardized protocols (ATCC). NRVMs were isolated on post-natal day (P) 1 as previously described (Lim et al., 2004). Hearts from 1-day-old Sprague Dawley pups were harvested and the atria removed. The ventricles were minced and subjected to trypsin digestion (0.6 mg/ml; Invitrogen) followed by a second digestion with collagenase type II (1 mg/ml; Worthington). NRVMs were obtained by preplating the digested cell suspension to remove non-myocytes and the semi-purified cardiomyocytes were then plated on laminin-coated plates. Cardiomyocytes were grown at 37°C with 5% CO_2 in a humidified incubator in low glucose DMEM and 7% fetal bovine serum.

Cardiomyocyte quantification and proliferation *in vivo*

Zebrafish embryos carrying a *cmlc2*:GFP transgene were injected with control or *nppa*/*nppb* morpholino at the one-cell stage. The HS:*nppb* dual transgenic embryos also have a *cmlc2*:CFP fluorescent marker. At 48 hpf, the embryos were euthanized, their hearts were excised and fixed in 4% PFA for 12 hours at 4°C. The embryos were transferred to PBS and stored at 4°C. DAPI stain was applied, and the hearts were imaged using a Zeiss LSM5 Pascal confocal microscope. The nuclei of the CFP-positive cells were then counted using ImageJ software. Cardiomyocyte proliferation in zebrafish was assessed using a modified BrdU (5-bromo-2′-deoxyuridine) protocol (Lazic and Scott, 2011). Briefly, 48 hpf *cmlc2*:GFP zebrafish embryos were bathed in 10 mM BrdU for 30 minutes with 15% DMSO on an ice bath, then placed in a 28°C incubator for 3.5 hours. Embryos were then fixed in 4% PFA for 60 minutes, and washed in PBST. The embryos were then placed in acetone for 10 minutes, washed and bleached. A primary antibody directed against BrdU (G3G4, DSHB) was then used to detect BrdU incorporation. Secondary antibody was Alexa 568-conjugated goat anti-mouse (A11004, Invitrogen). To detect CFP-positive cardiomyocytes an Alexa 488-conjugated anti-GFP antibody was utilized (A21311, Invitrogen).

Assessment of zebrafish ventricular cardiomyocyte differentiation between 30 to 48 hpf

Dual transgenic embryos [*cmlc2*:GAL4 x UAS:kaede (Scott et al., 2007)] (30 hpf) were anesthetized and mounted in 1% methylcellulose on a bridge slide, and exposed to 330-385 nm light on a Olympus FV1000 confocal microscope. Fine focus was used to scan the light through the entire plane of the heart, and embryos were examined under FITC and Cy3 filters to show photoconversion from green to red. Embryos were then removed from the methylcellulose and allowed to grow to 48 hpf in E3. At 48 hpf, they were mounted in 1% methylcellulose containing tricaine and were imaged on the FV1000 confocal microscope.

Cardiomyocyte quantification and proliferation *in vitro*

Cells were manually counted using a hemocytometer and plated into a 96-well microtiter plate. After the cells adhered to the plate bottom they were washed with PBS and a DNA-binding reagent (Cyquant NF, Invitrogen) was added to a subset of the wells to obtain a baseline (0 hour) measurement. Fluorescence in the wells was measured using a microtiter plate reader (Spectramax M5) at 485-nm excitation and 530-nm emission settings. The remaining wells on the plate were then exposed to peptides or small molecules at varying concentrations for the next 48 hours. After 48 hours of exposure, the exposed wells were washed with PBS and the DNA-binding reagent was added and measured on a fluorescent microtiter plate reader. In order to convert fluorescence values to cell number, we did triplicate cell counts manually using a hemocytometer and plated a range of 500 to 6000 cells/well. After cell adherence, the plates were measured and a formula [530 nm emission=0.0605(cell count) + 1.4532] was derived using linear regression (R^2=0.9998) to convert raw fluorescence values to cell number in subsequent experiments.

To measure the number of NRVMs in S phase of the cell cycle, we incubated the cells with 5-ethynyl-2′-deoxyuridine (EdU; Invitrogen) for 5 hours after the initial 48-hour exposure to the specified concentrations of ANP peptide. The cells were then fixed with 4% PFA and permeabilized with 0.5% Triton X-100. EdU detection was performed using Alexa Fluor 594-conjugated azide (A10270, Invitrogen). To selectively label cardiomyocytes, we incubated the fixed NRVMs in either a monoclonal antibody specific for cardiac Troponin T (ab10214, Abcam) or sarcomeric alpha actinin (ab9465, Abcam). Detection of the primary mouse monoclonal antibodies was performed using Alexa Fluor 488-labeled goat-anti mouse

secondary antibodies (A11029, Invitrogen). Imaging was performed on either confocal microscope (Zeiss LSM510) or upright fluorescence microscope (Zeiss Axioplan 2). The number of EdU-positive and cardiac troponin T dual-positive cells were then manually counted and divided by the total number of cardiac troponin T-positive cells.

Apoptosis assessment

Apoptosis assessment *in vitro* was performed using Annexin V and TUNEL assessment on proliferating NRVMs exposed to ANP. Primary NRVMs were cultured and exposed to ANP for 48 hours. The cells were then washed and exposed to Annexin V-Alexa Fluor 488 conjugate (Invitrogen, A13201) and propodium iodide. The cells were sorted using a BD FACSAria II with an average of 10,000 counts/biological replicate with three biological replicates for each treatment group. For the TUNEL assessment, NRVMs were cultured and exposed to ANP for 48 hours and then fixed with 1% PFA on ice for 15 minutes and stored in 70% (v/v) ethanol at $-20°C$ for 48 hours. The cells were then washed, labeled with BrdU labeling solution and then stained with Alexa Fluor 488-labeled anti-BrdU antibody (Invitrogen, A23210). The labeled cells were then analyzed by flow cytometry as described above. Acridine Orange staining was performed to determine the number of apoptotic cells in the zebrafish heart. Zebrafish embryos that had normal or increased expression of Nppb were exposed to 2 μg/ml of Acridine Orange for 30 minutes and anesthetized with tricaine. The embryos were then imaged using a fluorescence dissecting microscope (Olympus SZX12). The number of Acridine Orange-positive heart cells was then manually counted.

Microarray dataset analysis

Repository gene expression data were obtained from the Gene Expression Omnibus (http://www.ncbi.nlm.nih.gov/geo/; for accession numbers, see supplementary material Table S1). Data sets that analyzed purified cardiomyocyte samples were included for analysis. Each data set was separately normalized using robust multi-array average (RMA) for Affymetrix data or quantile normalization followed by log2 transformation for the non-Affymetrix data sets. Only the experimental channel was used for the Agilent two-color array data. To compare receptor expression across studies, normalized log2 hybridization signal value ratios were calculated using two different internal housekeeping genes (*Gapdh* and *Actb*), which generated similar values. Only cardiomyocyte data sets that expressed high levels of cardiac troponin T (*Tnnt2*) were considered acceptable for further analysis. Likewise, we used endothelial cell expression data to serve as a negative control to verify that *Tnnt2* expression could adequately differentiate between cardiomyocyte and non-cardiomyocyte populations.

Peptides and small molecules

The following peptides and small molecules were used: atrial natriuretic peptide (ANP) (0.5-10,000 nM; Anaspec, 20652); C-type natriuretic peptide (CNP) (1-10,000 nM; Phoenix Pharmaceuticals, 012-03); dendroaspis natriuretic peptide (DNP) (0.1-1000 nM; Phoenix Pharmaceuticals, 013-01); AP-811 (10-500 nM; California Peptide Research); 8-Br-cAMP (1-100 μM; Santa Cruz Biotech, sc-201564); Rp-8-pCPT-cGMP (1 μM; Enzo, BML-CN206-0001); 8-pCPT-cGMP (100-800 μM; Sigma, C5438); SQ 22536 (250 nM-5 μM; Santa Cruz Biotech, sc-201572); isoproterenol (1 μM; Sigma, I6504); and KT 5823 (1 nM; Tocris, 1289).

Statistics

All data displayed as mean ± s.e.m. unless otherwise noted. Data were analyzed using Student's *t*-test for comparisons between two groups or one-way ANOVA for comparisons between three or more groups. Significance was defined as $P<0.05$.

Supplementary material
Supplementary material available online at
http://dev.biologists.org/lookup/suppl/doi:10.1242/dev.100370/-/DC1

References

Anand-Srivastava, M. B., Sehl, P. D. and Lowe, D. G. (1996). Cytoplasmic domain of natriuretic peptide receptor-C inhibits adenylyl cyclase. Involvement of a pertussis toxin-sensitive G protein. *J. Biol. Chem.* **271**, 19324-19329.

Bloch, K. D., Seidman, J. G., Naftilan, J. D., Fallon, J. T. and Seidman, C. E. (1986). Neonatal atria and ventricles secrete atrial natriuretic factor via tissue-specific secretory pathways. *Cell* **47**, 695-702.

Choi, W. Y., Gemberling, M., Wang, J., Holdway, J. E., Shen, M. C., Karlstrom, R. O. and Poss, K. D. (2013). In vivo monitoring of cardiomyocyte proliferation to identify chemical modifiers of heart regeneration. *Development* **140**, 660-666.

de Bold, A. J. (1985). Atrial natriuretic factor: a hormone produced by the heart. *Science* **230**, 767-770.

Hammoud, L., Burger, D. E., Lu, X. and Feng, Q. (2009). Tissue inhibitor of metalloproteinase-3 inhibits neonatal mouse cardiomyocyte proliferation via EGFR/JNK/SP-1 signaling. *Am. J. Physiol.* **296**, C735-C745.

Holtwick, R., van Eickels, M., Skryabin, B. V., Baba, H. A., Bubikat, A., Begrow, F., Schneider, M. D., Garbers, D. L. and Kuhn, M. (2003). Pressure-independent cardiac hypertrophy in mice with cardiomyocyte-restricted inactivation of the atrial natriuretic peptide receptor guanylyl cyclase-A. *J. Clin. Invest.* **111**, 1399-1407.

Horsthuis, T., Houweling, A. C., Habets, P. E., de Lange, F. J., el Azzouzi, H., Clout, D. E., Moorman, A. F. and Christoffels, V. M. (2008). Distinct regulation of developmental and heart disease-induced atrial natriuretic factor expression by two separate distal sequences. *Circ. Res.* **102**, 849-859.

John, S. W., Krege, J. H., Oliver, P. M., Hagaman, J. R., Hodgin, J. B., Pang, S. C., Flynn, T. G. and Smithies, O. (1995). Genetic decreases in atrial natriuretic peptide and salt-sensitive hypertension. *Science* **267**, 679-681.

Johns, D. G., Ao, Z., Heidrich, B. J., Hunsberger, G. E., Graham, T., Payne, L., Elshourbagy, N., Lu, Q., Aiyar, N. and Douglas, S. A. (2007). Dendroaspis natriuretic peptide binds to the natriuretic peptide clearance receptor. *Biochem. Biophys. Res. Commun.* **358**, 145-149.

Kerkela, R., Kockeritz, L., Macaulay, K., Zhou, J., Doble, B. W., Beahm, C., Greytak, S., Woulfe, K., Trivedi, C. M., Woodgett, J. R. et al. (2008). Deletion of GSK-3beta in mice leads to hypertrophic cardiomyopathy secondary to cardiomyoblast hyperproliferation. *J. Clin. Invest.* **118**, 3609-3618.

Khambata, R. S., Panayiotou, C. M. and Hobbs, A. J. (2011). Natriuretic peptide receptor-3 underpins the disparate regulation of endothelial and vascular smooth muscle cell proliferation by C-type natriuretic peptide. *Br. J. Pharmacol.* **164**, 584-597.

Langenickel, T. H., Buttgereit, J., Pagel-Langenickel, I., Lindner, M., Monti, J., Beuerlein, K., Al-Saadi, N., Plehm, R., Popova, E., Tank, J. et al. (2006). Cardiac hypertrophy in transgenic rats expressing a dominant-negative mutant of the natriuretic peptide receptor B. *Proc. Natl. Acad. Sci. USA* **103**, 4735-4740.

Lazic, S. and Scott, I. C. (2011). Mef2cb regulates late myocardial cell addition from a second heart field-like population of progenitors in zebrafish. *Dev. Biol.* **354**, 123-133.

Lelièvre, V., Hu, Z., Ioffe, Y., Byun, J. Y., Flores, A., Seksenyan, A. and Waschek, J. A. (2006). Paradoxical antagonism of PACAP receptor signaling by VIP in Xenopus oocytes via the type-C natriuretic peptide receptor. *Cell. Signal.* **18**, 2013-2021.

Li, F., Wang, X., Capasso, J. M. and Gerdes, A. M. (1996). Rapid transition of cardiac myocytes from hyperplasia to hypertrophy during postnatal development. *J. Mol. Cell. Cardiol.* **28**, 1737-1746.

Li, Y., Madiraju, P. and Anand-Srivastava, M. B. (2012). Knockdown of natriuretic peptide receptor-A enhances receptor C expression and signalling in vascular smooth muscle cells. *Cardiovasc. Res.* **93**, 350-359.

Lim, C. C., Zuppinger, C., Guo, X., Kuster, G. M., Helmes, M., Eppenberger, H. M., Suter, T. M., Liao, R. and Sawyer, D. B. (2004). Anthracyclines induce calpain-dependent titin proteolysis and necrosis in cardiomyocytes. *J. Biol. Chem.* **279**, 8290-8299.

Matsukawa, N., Grzesik, W. J., Takahashi, N., Pandey, K. N., Pang, S., Yamauchi, M. and Smithies, O. (1999). The natriuretic peptide clearance receptor locally modulates the physiological effects of the natriuretic peptide system. *Proc. Natl. Acad. Sci. USA* **96**, 7403-7408.

McKoy, G., Bicknell, K. A., Patel, K. and Brooks, G. (2007). Developmental expression of myostatin in cardiomyocytes and its effect on foetal and neonatal rat cardiomyocyte proliferation. *Cardiovasc. Res.* **74**, 304-312.

Murthy, K. S. and Makhlouf, G. M. (1999). Identification of the G protein-activating domain of the natriuretic peptide clearance receptor (NPR-C). *J. Biol. Chem.* **274**, 17587-17592.

Nir, A., Zhang, D. F., Fixler, R., Burnett, J. C., Jr, Eilam, Y. and Hasin, Y. (2001). C-type natriuretic peptide has a negative inotropic effect on cardiac myocytes. *Eur. J. Pharmacol.* **412**, 195-201.

Nussenzveig, D. R., Lewicki, J. A. and Maack, T. (1990). Cellular mechanisms of the clearance function of type C receptors of atrial natriuretic factor. *J. Biol. Chem.* **265**, 20952-20958.

O'Tierney, P. F., Chattergoon, N. N., Louey, S., Giraud, G. D. and Thornburg, K. L. (2010). Atrial natriuretic peptide inhibits angiotensin II-stimulated proliferation in fetal cardiomyocytes. *J. Physiol.* **588**, 2879-2889.

Oliver, P. M., Fox, J. E., Kim, R., Rockman, H. A., Kim, H. S., Reddick, R. L., Pandey, K. N., Milgram, S. L., Smithies, O. and Maeda, N. (1997). Hypertension, cardiac hypertrophy, and sudden death in mice lacking natriuretic peptide receptor A. *Proc. Natl. Acad. Sci. USA* **94**, 14730-14735.

Robu, M. E., Larson, J. D., Nasevicius, A., Beiraghi, S., Brenner, C., Farber, S. A. and Ekker, S. C. (2007). p53 activation by knockdown technologies. *PLoS Genet.* **3**, e78.

Scott, E. K., Mason, L., Arrenberg, A. B., Ziv, L., Gosse, N. J., Xiao, T., Chi, N. C., Asakawa, K., Kawakami, K. and Baier, H. (2007). Targeting neural circuitry in zebrafish using GAL4 enhancer trapping. *Nat. Methods* **4**, 323-326.

Scott, N. J., Ellmers, L. J., Lainchbury, J. G., Maeda, N., Smithies, O., Richards, A. M. and Cameron, V. A. (2009). Influence of natriuretic peptide receptor-1 on survival and cardiac hypertrophy during development. *Biochim. Biophys. Acta* **1792**, 1175-1184.

Sudoh, T., Kangawa, K., Minamino, N. and Matsuo, H. (1988). A new natriuretic peptide in porcine brain. *Nature* **332**, 78-81.

Suga, S., Nakao, K., Hosoda, K., Mukoyama, M., Ogawa, Y., Shirakami, G., Arai, H., Saito, Y., Kambayashi, Y., Inouye, K. et al. (1992). Receptor selectivity of natriuretic peptide family, atrial natriuretic peptide, brain natriuretic peptide, and C-type natriuretic peptide. *Endocrinology* **130**, 229-239.

Tamura, N., Ogawa, Y., Chusho, H., Nakamura, K., Nakao, K., Suda, M., Kasahara, M., Hashimoto, R., Katsuura, G., Mukoyama, M. et al. (2000). Cardiac fibrosis in mice lacking brain natriuretic peptide. *Proc. Natl. Acad. Sci. USA* **97**, 4239-4244.

Tanaka, M., Chen, Z., Bartunkova, S., Yamasaki, N. and Izumo, S. (1999). The cardiac homeobox gene Csx/Nkx2.5 lies genetically upstream of multiple genes essential for heart development. *Development* **126**, 1269-1280.

Thisse, C. and Thisse, B. (2008). High-resolution in situ hybridization to whole-mount zebrafish embryos. *Nat. Protoc.* **3**, 59-69.

Veale, C. A., Alford, V. C., Aharony, D., Banville, D. L., Bialecki, R. A., Brown, F. J., Damewood, J. R., Jr, Dantzman, C. L., Edwards, P. D., Jacobs, R. T. et al. (2000). The discovery of non-basic atrial natriuretic peptide clearance receptor antagonists. Part 1. *Bioorg. Med. Chem. Lett.* **10**, 1949-1952.

William, M., Hamilton, E. J., Garcia, A., Bundgaard, H., Chia, K. K., Figtree, G. A. and Rasmussen, H. H. (2008). Natriuretic peptides stimulate the cardiac sodium pump via NPR-C-coupled NOS activation. *Am. J. Physiol.* **294**, C1067-C1073.

Zeller, R., Bloch, K. D., Williams, B. S., Arceci, R. J. and Seidman, C. E. (1987). Localized expression of the atrial natriuretic factor gene during cardiac embryogenesis. *Genes Dev.* **1**, 693-698.

Development